Journal of Chromatography A, 659 (1994) 403–415
Elsevier Science B.V., Amsterdam

CHROM. 25 540

Computational simulation of migration and dispersion in free capillary zone electrophoresis

I. Description of the theoretical model

J.C. Reijenga*

Department of Chemical Engineering, Eindhoven University of Technology, P.O. Box 513, 5600 MB Eindhoven (Netherlands)

E. Kenndler

Institute of Analytical Chemistry, University of Vienna, Währingerstrasse 38, A-1090 Vienna (Austria)

(First received May 10th, 1993; revised manuscript received September 6th, 1993)

ABSTRACT

An instrument simulator was developed for high-performance capillary electrophoresis which allows for fast graphic illustration of the effect of a large number of variables on the shape of the electropherogram. The input data of the separands are values of pK and mobilities at 25°C and infinite dilution. The instrument parameters that can be varied include capillary material, lengths, inside diameter, wall thickness, zeta potential, cooling temperature, voltage, polarity and open or closed mode. Hydrostatic injection is simulated, using time and pressure as variables. The following properties of the buffer can be varied: pH, ionic strength and effective mobility of background electrolyte ions. The effective mobilities are corrected for temperature and concentration effects. Extra-column effects from injection and detection are taken into account, and also peak dispersion arising from electroosmosis, diffusion, electromigration and heat production.

INTRODUCTION

The theoretical basis of electrophoretic separation has been extensively dealt with in the past. All phenomena occurring during separation were described either by exact mathematical relationships derived from the equation of continuity and other differential equations, or by empirical relationships verified experimentally and found to be valid under certain conditions. Many workers have contributed to this knowledge. For a historical overview, many excellent reviews and textbooks are available [1–9].

The introduction of advanced instrumentation (in part based on theoretical models) and the more recent use of microcomputers have made it possible to verify experiment and theory in a very efficient way. Computer programs have been written to simulate and verify many aspects of the theory [10–13], thus making it possible to refine the theoretical basis and extend the understanding of the phenomena. Even a unified model of the transient state phenomena of all possible electrophoretic configurations was put together in one computer program [10]. One is thus able to study the effects concerned in detail without actually performing experiments. The fundamental aspects consequently are accessible to all experienced researchers in the field.

* Corresponding author.

0021-9673/94/$07.00
SSDI 0021-9673(93)E0959-X

In addition to the textbooks mentioned, a number of workers have published on model refinement in capillary electrophoresis in recent years, especially with respect to a number of on-column dispersive effects [14–18], extra-column effects [19–21], concentration overload [22,23] and stacking effects [24–26].

In order to clarify the purpose of the present investigation, computer programs simulating instrumental separation techniques are classified into the following three categories, each with its own aim and requirements.

(I) Fundamental. The model in the program should be exact in every detail, describing the dynamics of the electrophoretic process in both transient and steady states.

(II) Optimization. The program should be fast and provide a fairly accurate prediction of the separation based on literature values and one's own previous experiments.

(III) Instruction. The program must be fast, flexible, very user-friendly and have graphics output and a reasonably predictive value.

Consideration of the requirements mentioned will lead to the obvious conclusion that some are contradictory. It was the aim of this study to simulate the final result of the electrophoretic process (categories II and III), depicted by the electropherogram, rather than to illustrate the dynamics in detail (category I). For this purpose, the two processes that determine the electrophoretic result, migration and dispersion, were simulated. A distinction was made between open and closed systems. The latter are not commercially available but clearly offer advantages that justify separate treatment [27].

The migration time was simply derived from the apparent mobilities, consisting of the effective mobilities of the separands and the electroosmotic mobility of the bulk liquid, both at given ionic strength and pH. To describe the effect on peak distortion, the plate height model was used, whereby the expressions for the plate height originating from different sources, as described in the literature, were taken but they were also modified and reformulated in a number of cases.

It was shown that a number of expressions for the different contributions to the total plate height contain the ratio of the effective mobility and the sum of the effective mobility and the electroosmotic mobility, which leads to the introduction of a dimensionless parameter, the electromigration factor. The influence of this factor on migration and dispersion will be discussed for both anions and cations. All important factors influencing the result were taken into account. These include instrument variables such as capillary material and dimensions, voltage, current and temperature. The physico-chemical properties of the buffer and the sample form the basis of the calculations. Extra-column effects arising from injection (overload, stacking) and detection (slit width and time constant) are included, in addition to dispersive effects resulting from diffusion, electroosmosis, electromigration and heat production.

EXPERIMENTAL

Programming environment

The software was written in QuickBasic version 4.5 (Microsoft, Redmond, WA, USA) using an IBM PC-compatible clone with a Model 386 processor, 4 Mbyte RAM, 100 Mbyte hard disk, 40 MHz clock speed and a 14-in. (1 in. = 2.54 cm) VGA colour monitor. In contrast to this, the computer program requires as a minimum hardware configuration: IBM XT-compatible PC, 8 MHz clock speed, 640 kbyte RAM, a 360 kbyte disk drive and a graphics monitor. The program automatically adjusts to Hercules, AT&T, CGA, EGA and VGA graphics. A numeric coprocessor is supported if present and emulated otherwise. A mouse (Microsoft mode) is optional. With a command line option, the program can also be run from a computer network, especially useful for training purposes.

The time necessary to calculate and display a typical electropherogram is in the range of a few seconds. The user interface, consisting of pull-down menus, to be activated by single-letter commands, cursor movements or the mouse, is much the same as in a previously developed simulator for gas chromatography [28].

Details on the availability of the program can be obtained from the first author request.

Data file

A data file CEDATA.DAT of pK and mobility values was made, consisting of previously

published data [6,29–31]. These data generally refer to 25°C and infinite dilution. The simulation program itself can be used to edit the CEDATA.DAT or any other data file (change values, add new components). In this way the simulator can also work with user-defined databases.

Generation of electropherogram

Each calculation of retention and dispersion is followed by the generation and display of a new electropherogram, see Fig. 1 for the screen layout. First, a noisy baseline is generated. Then peaks are generated over an interval of three standard deviations on both sides of the maximum, convoluted with a triangular moving average filter due to concentration overload and, after multiplication with a response factor, added to the baseline. In order to facilitate visual interpretation, both detector amplitude and time axes can be varied.

DISCUSSION OF THE THEORETICAL MODEL

The theoretical model is based on the calculation of the migration and dispersion of the individual separands. It consists of a number of equations which are dealt with in previous publications. In several instances, the equations were reformulated and presented in a uniform manner. For all equations, dimension analysis was applied in order to check the various steps involved in their derivation. However, they are included in the present contribution as the simulation model should be described exactly in order to make transparent the capabilities and limitations of the program.

Calculations of instrument variables and temperature effects

In the electrophoresis simulator, the following calculations are carried out each time a parameter is changed and consequently a new electropherogram is calculated, see Table I for an overview of these parameters. The field strength E (V m^{-1}) is first calculated from the constant voltage U (V) of the electrode at the injection side and the overall capillary length L_0 (m):

$$E = U/L_0 \quad (1)$$

Both U and E are signed quantities. The subsequent calculation of the driving current, power dissipation, temperature and specific conductivity requires an iteration because of the temperature dependence of mobility and conductivity. An estimate of the current is made first, assuming that the temperature in the capillary is equal to the cooling temperature. Then the buffer

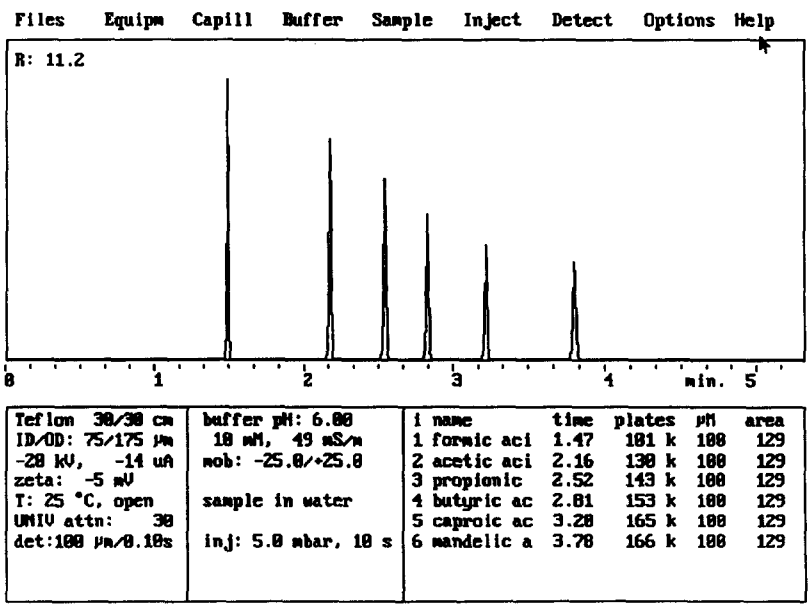

Fig. 1. Typical screen of the simulator with equipment parameters on the lower left-hand side and sample parameters on the lower right-hand side. An electropherogram is shown of signal amplitude *vs.* time.

TABLE I

MENU STRUCTURE OF THE COMPUTER PROGRAM HPCESIM

Files	Load	Equip, Buffer, Sample, pheroGram
	Save	Equip, Buffer, Sample, pheroGram
	Print	some hints on screen printing
	Edit_data	edits the data base
	Reload_data	reloads data base if data were altered
	Quit	Yes, No
Equipm	Voltage	1..35 kV
	Mode	Open, Closed
	Polarity	Positive, Negative
	Temperature	0..40°C (cooling temperature)
Capill	length Detector	50..500 mm
	Overall_length	50..500 mm
	Internal_diam.	5..200 μm
	Wall_thickness	10..200 μm
	Material	Teflon, Glass, Quartz
	Zeta potential	-200..+200 mV
Buffer	pH	2.00..12
	Ionic_strength	0.002..0.1 mol/l
	Anion_mob.	$-1..-99.10^{-9}$ $m^2V^{-1}s^{-1}$
	Cation_mob.	$+1..+99.10^{-9}$ $m^2V^{-1}s^{-1}$
Sample	Add	up to 6 (VGA: 8) components per sample
	Concentration	1..500 μmol/l
	Delete	any sample component
	Solvent	Water, Buffer
Inject	Pressure	10..300 Nm^{-2}
	Time	1..20 s
Detect	Response	Universal, Conductivity
	Attenuation	1-3000
	Slit_width	10..500 μm (aperture)
	Time_constant	0.01..1 s
	Interval	60 s..40 min.
Options	Erase	Auto, Off (superimpose signals)
	Vary	pH, Voltage, Ionic strength
	Noise	0.1..10
	Model_data	shows plate heights, resolutions, etc
	Sample_data	shows valence, pK's, mobilities
	Alter_data	valence 1..4
		pK -5..+14
		mobility $-99..+99.10^{-9}$ $m^2V^{-1}s^{-1}$
Help		

temperature in the capillary is calculated from the power dissipation. Finally, the driving current is again calculated using temperature-corrected conductivity (a temperature dependence of 2.5% per degree is taken). The iteration is repeated until the buffer-specific conductivity remains constant within 0.1%.

The iteration is carried out as follows: neglecting the contribution from H^+ and OH^-, the specific conductivity of the buffer κ (S m^{-1}) is calculated from the ionic strength I (mol l^{-1}):

$$\kappa = 10^3 FI(|u_{\text{eff,A}}| + |u_{\text{eff,B}}|) \quad (2)$$

where F is the Faraday constant (96 500 C mol^{-1}) and $u_{\text{eff,A}}$ and $u_{\text{eff,B}}$ are the effective mobility of the co-ion A and counter ion B in the background electrolyte, respectively (m^2 V^{-1} s^{-1}). For pH < 4, an additional contribution from H_3O^+ is included. The driving current i (A), having the same sign as E, follows from

$$i = \pi\kappa R_i^2 E \quad (3)$$

where R_i is the inner radius (m) of the capillary of circular cross-section.

For the calculation of the average temperature T (K) in the capillary, one first needs the temperature T_w at the inner wall. This temperature can be calculated [3] from the cooling temperature T_0 using

$$T_w = T_0 + \frac{\kappa E^2 R_i^2}{2} \cdot \frac{1}{\lambda_c} \cdot \ln\left(\frac{R_0}{R_i}\right) \quad (4)$$

where R_0 is the outside radius (m) of the capillary and λ_c the thermal conductivity of the capillary material (W m^{-1} K^{-1}). This relationship assumes a capillary that is not coated on either side. The coating normally used in capillary zone electrophoresis (CZE) with fused-silica capillaries, however, does not significantly influence their thermal properties. No limitation to heat transfer on either side of the capillary wall was assumed. Forced cooling on the outside is needed to keep this assumption reasonable.

The average temperature T in the capillary is now obtained by integration:

$$T = \frac{1}{\pi R_i^2} \int_{r=0}^{R_i} 2\pi r T(r)\, dr \quad (5)$$

where $T(r)$ is the radial temperature profile:

$$T(r) = T_w + \frac{\kappa E^2 R_i^2}{4\lambda_s}\left(1 - \frac{r^2}{R_i^2}\right) \quad (6)$$

where λ_s is the thermal conductivity of the solution (W m^{-1} K^{-1}).

Integration of the former and combination with eqn. 4 yields the following relationship for the average temperature:

$$T = T_0 + \kappa E^2 R_i^2 \left[\frac{1}{2\lambda_c} \cdot \ln\left(\frac{R_0}{R_i}\right) + \frac{1}{8\lambda_s}\right] \quad (7)$$

Integration assumes a radially constant κ, a second-order effect. In a given configuration (R_0,

R_i, λ_c and λ_s) the temperature rise $(T - T_0)$ is proportional to κE^2.

After the iterative calculation of temperature and driving current, a number of other variables, which are independent of the separands, are calculated.

Migration

Effects due to finite electrolyte concentration. As the mobilities of the database refer to zero concentration, a correction for the ionic strength of the buffer is necessary. This requires more data on the separands than are normally available (ionic radius, etc.), whereas the simpler models describing concentration dependence are usually valid only up to 0.001 mol l^{-1}. Above this concentration, more sophisticated correction factors are usually necessary. This is all beyond the aim of the present simulation. However, in the co-migration of monovalent and multivalent ions, the ionic strength of the buffer can contribute considerably to selectivity [4,6]. Therefore, an approximate dependence of mobility on ionic strength and effective charge has been included.

The following relationship [32], a charge-dependent exponential decrease in mobility as a function of the square root of the ionic strength I, was used to calculate the actual mobilities u_{act} from the absolute mobilities u_{abs}:

$$u_{act,j} = u_{abs,j} \exp\left(\frac{-\sqrt{I}}{2z_{e,j}^{-1.78}}\right) \quad (8)$$

where $z_{e,j}$ is absolute charge of the subspecies j.

Calculation of migration times. For each of the separands, the effective mobility u_{eff} is now calculated from pH and all i pK_j values and $i + 1$ actual mobilities $u_{act,j}$ of ions of valence i:

$$u_{eff} = u_{act,0} + \sum_{j=1}^{i} \frac{1}{1 + 10^{(pK_j - pH)}} \cdot (u_{act,j} - u_{act,j-1}) \quad (9)$$

where $u_{act,0}$ is the mobility at low pH values, corrected for the ionic strength. Negative species have a minus sign for u so that amphoteric separands can also be included.

In open systems, electroosmotic flow can play an important role in the resulting migration time. The ζ potential (V) of the capillary wall determines the electroosmotic mobility u_{eo} (m^2 V^{-1} s^{-1}):

$$u_{eo} = -\frac{\zeta \varepsilon}{\eta} \quad (10)$$

where ε is the dielectric constant of the buffer ($708 \cdot 10^{-12}$ F m^{-1} for water at room temperature) and η is the viscosity of the buffer (N m^{-2} s). The value for η in this relationship is corrected to the average temperature T with a temperature coefficient of -0.025 K^{-1}.

The ζ potential is introduced here as an independent variable, which requires some explanation. In actual practice, the ζ potential of the capillary material will depend on both the ionic strength and pH of the electrolyte in a complicated manner. The effects resulting from coating procedures and additives to the background electrolyte will add a further complication. In addition, the ζ potential may change both in time and in axial direction (sample introduction). All these effects are too dependent on unknown actual conditions to be able to simulate in a practicle manner. In the present simulator, the effects of electroosmosis, buffer ionic strength and pH and sample load can thus be investigated in a mutually independent way.

As was also pointed out in a previous paper [16], it will be shown here that the effective mobility relative to the total mobility plays an important role in migration and dispersion. For this reason, the dimensionless parameter electromigration factor f_{em} is introduced as the relative contribution of electrophoretic mobility to the total mobility:

$$f_{em} = \frac{u_{eff}}{u_{eff} + u_{eo}} \quad (11)$$

The effective electrophoretic and electroosmotic mobilities in this equation are signed quantities. A negative value of f_{em} can therefore be obtained. Physically it would mean an ion moving against the electroosmotic flow with a net velocity in the direction of electroosmosis. Whether such a separand would reach the detector depends on the sign of the field strength, electroosmosis and charge.

Now the migration time t_m(s) follows from u_{eff} and u_{eo}:

$$t_m = \frac{L_d}{E(u_{eo} + u_{eff})} = \frac{L_d f_{em}}{E u_{eff}} \quad \text{(open systems)} \tag{12}$$

$$t_m = \frac{L_d}{E u_{eff}} \quad \text{(closed systems)} \tag{12a}$$

where L_d is the length of the capillary to the detector. Only those separands with a positive sign of t_m will eventually reach the detector. Separands having a negative migration time move away from the detector and are not considered in subsequent calculations. Positive migration times occur if none or two of the variables f_{em}, E or u_{eff} is negative.

In the above and subsequent relationships where a distinction between open and closed systems was made, the electromigration factor f_{em} plays an essential role. It must be emphasized that in closed systems the value of f_{em} is not necessarily unity, although the net electroosmotic flow is compensated for by closing the system with a membrane or another device; u_{eo} is not zero unless other precautions such as surface modification are also taken.

Dispersion

Peak dispersion can be described by the plate height model. For the case that the individual contributions to peak broadening are independent of each other, their particular plate height H_i can be incrementally added, giving the total plate height [19]. The peak width, given by the second moment (the square of the standard deviation for the case of a Gaussian partition function) is related to H by $\sigma^2 = L_d H$, where σ is expressed in distance units in the capillary.

Two different types of contributions to peak broadening will be discussed in the following: those caused by extra-column effects [19–21], given by the finite width of injection and detector slit width and time constant, and those originating from the electrophoretic process [14–18], *i.e.*, longitudinal diffusion, heat generation and the occurrence of the profile of the electroosmotic flow. Concentration overload [22,23] and stacking [24–26] are also considered.

Extra-column effects of injection and detection. The applied sample injection volume V_{inj}(m^3) is

$$V_{inj} = \frac{\pi P R_i^4 t_{inj}}{8 L_0 \eta} \tag{13}$$

where P is the pressure drop (N m^{-2}) and t_{inj} the injection time (s). The η value in this case is corrected to the cooling temperature as injection takes place with the high voltage switched off. The amount injected is calculated from the separand concentration in the sample and V_{inj}.

Depending on the ionic strength of the sample (dissolved in buffer or in water), a stacking effect [24–26] is caused by the fact that the field strength in the sample compartment is different from that in the separation compartment. This field strength ratio is equal to the inverse of the specific conductivity ratio. This requires additional knowledge of sample counter ion types, pK values and concentrations and also sample pH. In order to circumvent this problem, this specific conductivity ratio is approximated by the ionic strength ratio, so that

$$\frac{E_s}{E} = \frac{I}{I_s} \tag{14}$$

where the subscript s indicates the non-adjusted sample plug. This relationship does not take into account effective mobility differences between the components present, including the effect of pH in the sample compartment. The ionic strength of the sample I_s is in turn approximated by the total concentration of sample components.

After stacking, the volume of the adjusted sample plug V_{st} is

$$V_{st} = V_{inj} \cdot \frac{I_s}{I} = \frac{\pi P R_i^4 t_{inj} I_s}{8 L_0 \eta I} \tag{15}$$

and the length δ_{inj}(m) of the cylindrical, stacked sample plug is

$$\delta_{inj} = \frac{V_{st}}{\pi R_i^2} = \frac{P R_i^2 t_{inj} I_s}{8 L_0 \eta I} \tag{16}$$

Assuming an initially rectangular concentration

profile [19], the plate height H_{inj} due to injection dispersion can be calculated by

$$H_{inj} = \frac{L_d}{12}\left(\frac{\delta_{inj}}{L_d}\right)^2 = \frac{\delta_{inj}^2}{12L_d} = \frac{P^2 R_i^4 t_{inj}^2 I_s^2}{768 L_d L_0^2 \eta^2 I^2} \quad (17)$$

The detector slit width δ_{det}(m), also assumed to be of a rectangular shape, determines the plate height in a way similar to the contribution from the injection:

$$H_{det} = \frac{L_d}{12}\left(\frac{\delta_{det}}{L_d}\right)^2 = \frac{\delta_{det}^2}{12L_d} \quad (18)$$

The dynamic response of the detector, expressed by the time constant τ(s) contributes as an exponential function to the total plate height [19], in which the respective migration times t_m can be substituted:

$$H_\tau = L_d\left(\frac{\tau}{t_m}\right)^2 = \frac{\tau^2 E^2 u_{eff}^2}{f_{em}^2 L_d} \quad \text{(open systems)} \quad (19)$$

$$H_\tau = L_d\left(\frac{\tau}{t_m}\right)^2 = \frac{\tau^2 E^2 u_{eff}^2}{L_d} \quad \text{(closed systems)} \quad (19a)$$

Longitudinal diffusion. The equation for the plate number H_{dif} due to diffusion in a longitudinal direction consists of

$$H_{dif} = L_d\left(\frac{\sigma_{dif}}{L_d}\right)^2 \quad (20)$$

The length-based variance σ_{dif}^2(m) due to longitudinal diffusion is given by the Einstein equation:

$$\sigma_{dif}^2 = 2Dt_m \quad (21)$$

In this equation, the diffusion coefficient D (m^2 s^{-1}) is replaced with the effective mobility u_{eff} with the Nernst–Einstein relationship:

$$D = \frac{u_{eff} RT}{z_e F} \quad (22)$$

where R is the gas constant (8.31 J mol^{-1} K^{-1}) and z_e is the overall effective charge of the separand.

Substitution of eqns. 12, 21 and 22 into eqn. 20 yields [16]

$$H_{dif} = \frac{2RT}{z_e EF} \cdot f_{em} \quad \text{(open systems)} \quad (23)$$

$$H_{dif} = \frac{2RT}{z_e EF} \quad \text{(closed systems)} \quad (23a)$$

In eqn. 23, z_e and E have opposite sign only for negative f_{em} values. The z_e value of each separand in the sample is obtained from the pH and the pK values of the subspecies:

$$z_e = z_0 - \sum_{j=1}^{n_i} \frac{1}{1 + 10^{(pK_j - pH)}} \quad (24)$$

where z_0 is the charge at low pH.

Thermal dispersion. Peak broadening due to thermal dispersion [3] is represented by the variance σ_T^2(m^2):

$$\sigma_T^2 = 2D_T t_m \quad (25)$$

The corresponding diffusivity D_T (m^2 s^{-1}), which substitutes the diffusion coefficient in the Einstein equation, was estimated by Virtanen [3]:

$$D_T = \frac{f_T^2 \kappa^2 u_{eff}^2 E^6 R_i^6}{3072 D \lambda_s^2} \quad (26)$$

where f_T is the temperature factor of κ and u [$(1/u)(\delta u/\delta T)$ (K^{-1})]. In this relationship, D is also converted into the effective mobility u_{eff} with eqn. 22. Using these equations, the plate height contribution due to thermal dispersion is derived as follows:

$$H_{ther} = L_d\left(\frac{\sigma_T}{L_d}\right)^2 = \frac{f_T^2 \kappa^2 E^6 R_i^6 z_e F}{1536 RT \lambda_s^2} \cdot \frac{u_{eff} t_m}{L_d}$$

$$H_{ther} = \frac{f_T^2 \kappa^2 E^5 R_i^6 z_e F}{1536 RT \lambda_s^2} \cdot f_{em} \quad \text{(open systems)} \quad (27)$$

$$H_{ther} = \frac{f_T^2 \kappa^2 E^5 R_i^6 z_e F}{1536 RT \lambda_s^2} \quad \text{(closed systems)} \quad (27a)$$

At first sight, the occurrence of the temperature T in the denominator may look strange as it would mean that H_{ther} would decrease with increasing temperature. At room temperature this effect is only 0.3% per degree. The temperature rise with respect to the thermostating tem-

perature is, however, proportional to κE^2, the proportionality constant follows from eqn. 7. As $\kappa^2 E^5$ is in the numerator, this clearly dominates the overall temperature dependence of H_{ther}. If the temperature coefficients of u_{em} and u_{eo} are taken to be of the same order of magnitude, f_{em} will be relatively independent of temperature. There are three coefficients in eqn. 27 which may have a negative sign: E^5, z_e and f_{em}. Their product will always be positive for those ions reaching the detector.

Electroosmotic dispersion. The dispersion due to electroosmosis is considered negligeable in open systems [2,3], assuming ideal plug flow, and therefore a hypothetical value of 10^{-9} m for H_{eo} is taken. In closed systems this is not the case, contributing the variance σ_{eo}^2 (m^2) by

$$\sigma_{eo}^2 = 2D_{eo}t_m \tag{28}$$

The corresponding diffusivity D_{eo} (m^2 s^{-1}) follows from

$$D_{eo} = \frac{R_i^2 u_{eo}^2 E^2}{48D} \tag{29}$$

The plate height H_{eo}, originating from electroosmotic dispersion, is calculated, again using the Nernst–Einstein relationship in order to replace the diffusion coefficient D, leading to

$$H_{eo} = L_d\left(\frac{\sigma_{eo}}{L_d}\right)^2 = \frac{R_i^2 u_{eo}^2 E^2 z_e F t_m}{24RTu_{eff}L_d} \tag{30}$$

Substitution of t_m by L_d/Eu_{eff} yields

$$H_{eo} = \frac{R_i^2 z_e EF}{24RT}\left(\frac{1}{f_{em}} - 1\right)^2 \tag{31}$$

The influence of the ζ potential is, of course, included in the electromigration factor f_{em}. Substitution of u_{eo} makes ζ more readily visible:

$$H_{eo} = \frac{R_i^2 \zeta^2 \varepsilon^2 z_e EF}{24RT\eta^2 u_{eff}^2} \tag{31a}$$

Electromigration dispersion (concentration overload). If the dispersion due to electromigration is considered [22,23], a triangular concentration distribution seems a fair approximation. The width of the triangle and the form (leading *vs.* tailing) are estimated as follows: the ratio of the effective mobility of the sample ($u_{eff,i}$) and that of the co-ion in the background electrolyte ($u_{eff,A}$) is first calculated:

$$r_i = \frac{u_{eff,i}}{u_{eff,A}} \tag{32}$$

The variables r_i, k_i and a_i were introduced by Mikkers *et al.* [22] to play a key role in electromigration dispersion of separand i. They are calculated as follows:

$$k_i = \frac{r_i - r_B}{(1 - r_B)r_i} \tag{33}$$

and

$$a_i = \frac{k_i(1 - r_i)}{I} \tag{34}$$

where r_B is the relative counter ion mobility, always negative as mobilities are signed quantities. Consequently, k_i is always positive. The sign of a_i designates either a leading or a tailing triangle. In order to avoid lengthy iterations, the mutual interference of the separand ions is limited to their contribution in the sample compartment.

When $r_i \neq 1$, the base width of the triangle δ_t can now be calculated [22], also using c_i, the non-adjusted separand concentration in the sample compartment:

$$\delta_t = |a_i|c_i\delta_{inj} + 2\sqrt{|u_{eff}Et_m a_i c_i \delta_{inj}|} \tag{35}$$

Considering both open (eqn. 12) and closed systems (eqn. 12a), it can be observed that shortly after switching on, the second term on the right-hand side of eqn. 33 will predominate, so that for closed systems:

$$\delta_t = 2\sqrt{|L_d a_i c_i \delta_{inj}|} \tag{35a}$$

This relationship was derived for electrophoresis in closed systems, assuming no additional dispersion. If, in open systems, the electroosmotic plug flow only changes t_m and the velocity of the front and the back of the triangle have equal velocity, the relationship can also apply in these cases, with the factor $|f_{em}|$ added under the square root sign.

To estimate the contribution of migration to the total dispersion, the migration effect is translated into the corresponding plate height [19], again only valid for $r_i \neq 1$ in open systems:

$$H_{conc} = \frac{L_d}{18}\left(\frac{\delta_t}{L_d}\right)^2 = \left|\frac{2a_i c_i \delta_{inj} f_{em}}{9}\right| \quad (36)$$

For closed systems, the migration time does not contain f_{em}, so

$$H_{conc} = \left|\frac{2a_i c_i \delta_{inj}}{9}\right| \quad (36a)$$

For the case where the effective mobility of the separand is equal to that of the co-ion in the background electrolyte ($r_i = 1$), δ_{inj} is the only additional contribution to the total Gaussian peak broadening, as mentioned above.

The triangular concentration distribution has an infinitely sharp (isotachophoretic) front for $r_i < 1$; for $r_i > 1$ it is sharp on the rear. The triangular concentration distribution is in fact an isotachophoretic sharpening effect that counteracts longitudinal diffusion. The approximation in the present simulation model is that these two effects are considered mutually independent, so that the plate height contributions are additive.

If all dispersive factors are considered independent, the corresponding variances are additive and the overall plate height H becomes

$$H = H_{inj} + H_{det} + H_\tau + H_{eo} + H_{ther} + H_{dif} + H_{conc}$$

Finally, substitution of the respective individual contributions yields the total plate height equation for free CZE in open systems:

$$H = \frac{P^2 R_i^4 t_{inj}^2 I_s^2}{768 L_d L_0^2 \eta^2 I^2} + \frac{\delta_{det}^2}{12 L_d} + \frac{\tau^2 E^2 u_{eff}^2}{f_{em}^2 L_d} + \frac{f_T^2 \kappa^2 E^5 R_i^6 z_e F}{1536 RT\lambda^2} \cdot f_{em} + \frac{2RT}{z_e EF} \cdot f_{em} + \left|\frac{2a_i c_i \delta_{inj} f_{em}}{9}\right| \quad (37)$$

and for closed systems:

$$H = \frac{P^2 R_i^4 t_{inj}^2 I_s^2}{768 L_d L_0^2 \eta^2 I^2} + \frac{\delta_{det}^2}{12 L_d} + \frac{\tau^2 E^2 u_{eff}^2}{L_d} + \frac{R_i^2 z_e EF}{24RT}\left(\frac{1}{f_{em}} - 1\right)^2 + \frac{f_T^2 \kappa^2 E^5 R_i^6 z_e F}{1536 RT\lambda^2} + \frac{2RT}{z_e EF} + \left|\frac{2a_i c_i \delta_{inj}}{9}\right| \quad (37a)$$

DISCUSSION

It is remarkable that several of these expressions include the electromigration factor f_{em} defined. As CZE is normally carried out in quartz capillaries, which exhibit a negative zeta potential, the electroosmotic mobility is consequently positive, the case on which the following discussion will be focused.

The dependence of f_{em} on the electrophoretic and electroosmotic mobility is fairly simple for cations, as shown in Fig. 2. Independent of the value of the electrophoretic mobility, f_{em} is unity for the case when no electroosmosis occurs. When electroosmosis does occur in the system, the factor f_{em} decreases with increasing electroosmotic mobility. In that case the effect of dispersion due to the three processes considered is reduced, which is obvious because sample components are transported through the separation capillary faster than without electroosmosis, and a shorter time is available for dispersion. As a consequence, the effect is more pronounced for cations with a low rather than a high effective mobility.

For anions the situation is more complex, as shown in Fig. 3. It can be seen that as for cations the value of f_{em} is unity in the absence of electroosmosis. In contrast to cations, f_{em} increases with increasing electroosmotic mobility for ions of a given mobility, very steeply when values for u_{eo} are approached which are similar to u_{eff}. For $u_{eo} = u_{eff}$, f_{em} is not defined: the electrophoretic velocity of the ion is exactly counterbalanced by the velocity of the electroosmotic flow, directed towards the cathode. Within the region under discussion, the plate height is always larger and the plate number smaller for anions with electroosmosis than without electroosmotic flow. If the value of u_{eo}

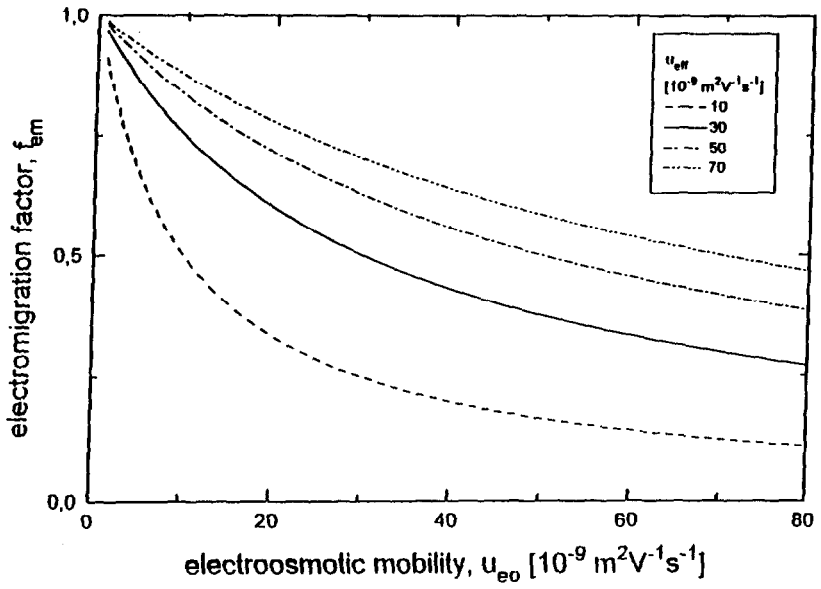

Fig. 2. Dimensionless electromigration factor f_{em} as a function of the electroosmotic mobility for cations at different electrophoretic mobilities.

exceeds that of u_{eff}, f_{em} becomes negative (the negative signs of f_{em} are always counterbalanced by negative signs of either z_e, E or U, as discussed previously, so that always positive plate height terms are obtained).

The absolute value of f_{em} therefore decreases steeply with increasing electroosmotic mobility and the corresponding plate heights also decrease. Here, the electric potential must be chosen positive, so that the ions are swept to the

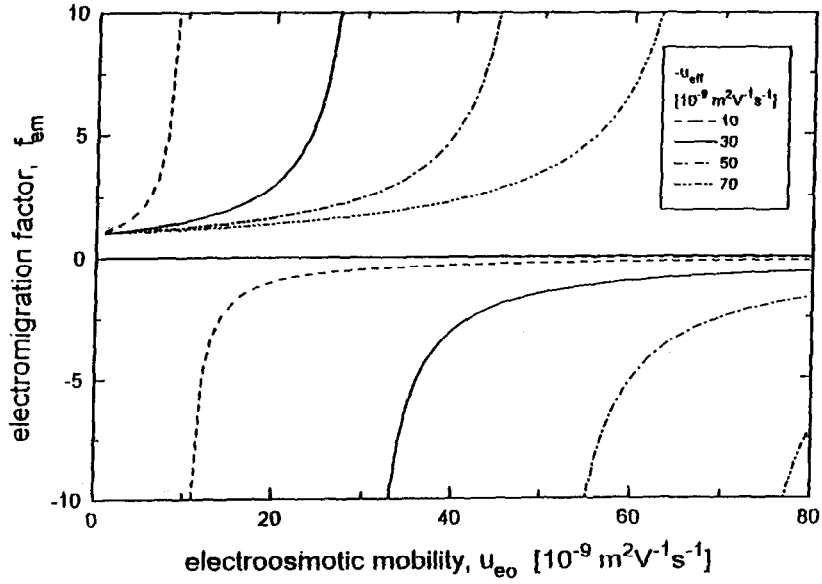

Fig. 3. Dimensionless electromigration factor f_{em} as a function of the electroosmotic mobility for anions at different electrophoretic mobilities.

cathode by electroosmosis. Within the entire range of u_{eo} the absolute value of f_{em} is larger than unity, which means that under those conditions the plate height is always larger than without electroosmosis. In contrast, the value of f_{em} is unity again when u_{eo} has twice the value of u_{eff}. For higher values of u_{eo}, f_{em} is smaller than unity, as for cations, and the plate heights are smaller than for the case without electroosmosis. This is clear because in this region the overall migration times (to the cathode side of the capillary) are finally smaller as for the case with pure electrophoretic migration, owing to the high velocity of the electroosmotic flow.

It should be pointed out, however, that the aim of CZE is the separation of components, and not only the generation of narrow peaks. Hence peak dispersion is only one side of the problem, and the effect of electroosmosis on the selectivity also has to be considered. It can be easily shown that, *e.g.*, for cations, the resolution is decreasing when electroosmosis occurs, despite the fact that the plate height is reduced. For anions again different regions can be distinguished. This problem has been discussed in more detail in a previous paper [16].

CONCLUSIONS

Migration model

The model of migration is straightforward; both electromigration and electroosmotic are taken into account. Concentration corrections for migration are applied in the form a simple approximation that already illustrates the importance of the ionic strength as a selectivity parameter. Temperature correction of mobilities is based on well known equations available in the literature. It is seen that the temperature rise in currently used capillaries can be kept to a minimum but that the thermostating temperature has a distinct influence on the migration times obtained. As the time axis is made variable between 1 and 40 min, the migration behaviour can be studied in a broad mobility range.

Dispersion model

All possible contributions to dispersion, except mutual interaction of separands during migration and adsorption, are considered. The contributions are given in the form of terms in a plate height equation. On a separate screen page, all plate height contributions are shown for the individual separands. Several, such as injection dispersion, other than caused by concentration overload, can under certain conditions be neglected with respect to others. Relating to detection dispersion (aperture, time constant), certain minimum instrumental requirements are easily calculated so that the detection can be optimized in this respect. Also, thermal dispersion can be controlled well enough. The model assumes that electroosmotic dispersion is only of importance in closed systems, with the electromigration factor f_{em} as a key parameter.

Limitations of the simulation

The predictive value of the model is of course limited, especially by the quality of the input data, the origin of which does not always describe in detail under what circumstances the mobilities and pK values were measured. In addition, the effect of concentration (ionic strength) is taken into account only in an approximate manner. The temperature coefficient for mobility is taken as 0.025 K^{-1} for all components whereas the pK values are assumed to be independent of temperature.

The behaviour of components is assumed to be independent of the presence of any other component, except for the properties of the buffer. In reality this is not always the case, but it is common practice to design an experiment in such a way that these matrix effects are limited.

As for the sample matrix effect during injection, sample pH and mutual interference between sample components are not taken into account. Also not included in the model are adsorption effects, leading to unsymmetric peaks and peak broadening due to different migration paths in coiled capillaries.

SYMBOLS

a_i	overload parameter (l mol^{-1})
c_i	non-adjusted separand concentration (mol l^{-1})
D	diffusion coefficient (m^2 s^{-1})

E field strength (V m^{-1})
f_{em} electromigration factor
f_T relative temperature coefficient for u (0.025) (K^{-1})
F Faraday constant (96 500) (C mol^{-1})
H overall plate height (m)
H_{inj} plate height due to injection (m)
H_{eo} plate height due to electroosmosis (m)
H_{dif} plate height due to diffusion (m)
H_{ther} plate height due to Joule heating (m)
H_τ plate height due to time constant (m)
H_{det} plate height due to detector slit width (m)
H_{conc} plate height due to concentration (m)
i current through capillary (A)
I ionic strength of buffer (mol l^{-1})
I_s ionic strength of sample (mol l^{-1})
k_i overload parameter
L_d length of capillary to detector (m)
L_0 overall length of capillary (m)
n_i valence of i
pH pH of buffer
pK_j pK of species j
P injection pressure (N m^{-2})
r distance from capillary axis (m)
r_i relative effective mobility of i
R gas constant (8.314) (J mol^{-1} K^{-1})
R_i inner radius of the capillary (m)
R_0 outer radius of the capillary (m)
t_{inj} injection time (s)
t_m migration time (s)
T_0 cooling temperature (K)
T_w temperature at inner wall (K)
T average temperature inside (K)
u_{eo} electroosmotic mobility (m^2 V^{-1} s^{-1})
u_{eff} effective electrophoretic mobility (m^2 V^{-1} s^{-1})
u_j absolute mobility of species j (m^2 V^{-1} s^{-1})
$u_{eff,A}$ effective mobility of co-ion (m^2 V^{-1} s^{-1})
$u_{eff,B}$ effective mobility of counter ion (m^2 V^{-1} s^{-1})
U voltage (V)
V_{inj} injected volume (m^3)
V_{sam} adjusted sample volume (m^3)
z_e effective charge number
z_0 charge at very low pH

α degree of dissociation
δ_{inj} adjusted sample length (m)
δ_{det} slit width of detector (m)
δ_t triangle width of zone (m)
ε dielectric constant ($708 \cdot 10^{-12}$) (F m^{-1})
κ specific conductivity of buffer (S m^{-1})
λ_s thermal conductivity of the solution (0.592) (W m^{-1} K^{-1})
λ_c thermal conductivity of the capillary (0.4–1.3) (W m^{-1} K^{-1})
η viscosity of buffer (0.0008904) (N m^{-2} s)
π constant (3.14159)
σ standard deviation (peak dispersion) (m)
σ_T^2 thermal dispersion variance (m^2)
σ_{eo}^2 electroosmotic dispersion variance (m^2)
τ time constant of the detector (s)
ζ zeta potential of the capillary (V)

REFERENCES

1 J.C. Giddings, in I.M. Kolthoff and P.J. Elving (Editors), *Treatise on Analytical Chemistry*, part I, Vol. 5, Wiley, New York, 1981, pp. 65–164.
2 S. Hjertén, *Chromatogr. Rev.*, 9 (1967) 122.
3 R. Virtanen, *Acta Polytech. Scand.*, 123 (1974) 1–67.
4 F.M. Everaerts, J.L. Beckers and Th.P.E.M. Verheggen, *Isotachophoresis —Theory, Instrumentation and Applications* (*Journal of Chromatography Library*, Vol. 7), Elsevier, Amsterdam, 1976.
5 J.W. Jorgenson and K.D. Lucaks, *Science*, 222 (1983) 266.
6 P. Bocek, M. Deml, P. Gebauer and V. Dolnik, *Analytical Isotachophoresis*, VCH, Weinheim, 1988.
7 F. Foret and P. Boček, in A. Chrambach, M.J. Dunn and B.J. Radola (Editors), *Advances in Electrophoresis*, *3*, VCH, Weinheim, 1989, pp. 273–342.
8 S. Hjertén, *Electrophoresis*, 11 (1990) 665.
9 S.F.Y. Li, *Capillary Electrophoresis —Principles, Practice and Applications* (*Journal of Chromatography Library*, Vol. 52), Elsevier, Amsterdam, 1992.
10 R.A. Mosher, D.A. Saville and W. Thormann, *The Dynamics of Electrophoresis*, VCH, Weinheim, 1992.
11 E.V. Dose and G.A. Guiochon, *Anal. Chem.*, 63 (1991) 1063.
12 J. Heinrich and H. Wagner, *Electrophoresis*, 13 (1992) 44.
13 H. Poppe, *J. Chromatogr.*, 506 (1990) 45.
14 F. Foret, M. Deml and P. Bocek, *J. Chromatogr.*, 452 (1988) 601.
15 E. Kenndler and Ch. Schwer, *Anal. Chem.*, 63 (1991) 2499.
16 Ch. Schwer and E. Kenndler, *Chromatographia*, 33 (1992) 331.
17 E. Kenndler and W. Friedl, *J. Chromatogr.*, 608 (1992) 161.
18 W. Friedl and E. Kenndler, *Anal. Chem.*, 65 (1993) 2003.
19 J. Sternberg, *Adv. Chromatogr.*, 2 (1966) 205–270.

20 K. Otsuka and S. Terabe, *J. Chromatogr.*, 480 (1989) 91.
21 X. Huang, W.F. Coleman and R.N. Zare, *J. Chromatogr.*, 480 (1989) 95.
22 F.E.P. Mikkers, F.M. Everaerts and Th.P.E.M. Verheggen, *J. Chromatogr.*, 169 (1979) 1.
23 H. Poppe, *Anal. Chem.*, 64 (1992) 1908.
24 B. Gas, J. Vacik and I. Zelensky, *J. Chromatogr.*, 545 (1991) 225.
25 P. Gebauer, W. Thormann and P. Bocek, *J. Chromatogr.*, 608 (1992) 47.
26 C. Schwer, B. Gas, W. Lottspeich and E. Kenndler, *Anal. Chem.*, 65 (1993) 2108.
27 Th.P.E.M. Verheggen and F.M. Everaerts, *J. Chromatogr.*, 638 (1993) 147.
28 J.C. Reijenga, *J. Chromatogr.*, 588 (1991) 217.
29 T. Hirokawa, M. Nishimo and Y. Kiso, *J. Chromatogr.*, 252 (1982) 49.
30 T. Hirokawa, M. Nishino, N. Aoki, Y. Kiso, Y. Sawamoto, T. Yagi and J.-I. Akiyama, *J. Chromatogr.*, 271 (1983) D1.
31 T. Hirokawa, Y. Kiso, B. Gas, I. Zuskova and J. Vacík, *J. Chromatogr.*, 628 (1993) 283.
32 J.C. Reijenga, *Internal Report*, University of Technology, Eindhoven, 1993.